Journal of Oceanology and Limnology

https://doi.org/10.1007/s00343-021-1046-5

Contrasting vertical distribution between prokaryotes and fungi in different water masses on the Ninety-East Ridge, Southern Indian Ocean*

Shujun LI[1, 2, #], Zhisong CUI[2, 3, #, **], Mutai BAO[1, **], Xiao LUAN[4], Fei TENG[2], Shujiang LI[2], Tengfei XU[2], Li ZHENG[2]

[1] *Frontiers Science Center for Deep Ocean Multispheres and Earth System*, *Key Laboratory of Marine Chemistry Theory and Technology*, *Ministry of Education*, *and College of Chemistry and Chemical Engineering*, *Ocean University of China*, *Qingdao 266100*, *China*

[2] *Marine Bioresources and Environment Research Center*, *First Institute of Oceanography*, *Ministry of Natural Resources of China*, *Qingdao 266061*, *China*

[3] *Laboratory for Marine Ecology and Environmental Science*, *Pilot National Laboratory for Marine Science and Technology* (*Qingdao*), *Qingdao 266237*, *China*

[4] *State Key Laboratory of Environmental Aquatic Chemistry*, *Research Center for Eco-Environmental Sciences*, *Chinese Academy of Sciences*, *Beijing 100085*, *China*

Received Oct. 19, 2020; accepted in principle Feb. 24, 2021; accepted for publication Apr. 1, 2021

Abstract Although the microbial diversity of the Indian Ocean has been extensively investigated, little is known about the community composition of microbes in the Southern Indian Ocean. In the present study, we divided 60 water column samples on the Ninety-East Ridge (NER) into five water masses according to the temperature-salinity curves. We presented, for the first time, a full description of the microbial biodiversity on NER through high-throughput amplicon sequencing approach, including bacteria, archaea, and fungi. We found that bacteria exhibited higher richness and diversity than archaea and fungi across the water masses on NER. More importantly, each water mass on NER featured distinct prokaryotic microbial communities, as indicated by the results of non-metric multidimensional scaling. In contrast, fungi were eurybathic across the water masses. Redundancy analysis results demonstrated that environmental factors might play a pivotal role in the formation and stability of prokaryotic communities in each water mass, especially that of archaea. In addition, indicator species might be used as fingerprints to identify corresponding water masses on NER. These results provide new insights into the vertical distribution, structure, and diversity of microorganisms on NER from the perspective of water mass.

Keyword: Ninety-East Ridge (NER); temperature-salinity curve; microbial vertical distribution; water mass; microbial diversity

1 INTRODUCTION

Microbes play a pivotal and fundamental role in the marine food web and global nutrient cycles (Arrigo, 2005; Fuhrman et al., 2015), participating in almost all oceanic biogeochemical processes. It is necessary to study the biodiversity of marine microbes before understanding their ecological role and function. To date, microbial diversity of the Indian Ocean has been extensively investigated (Sinha et al., 2019; Wang et al., 2021). However, little is known about the community composition of microbes in the Southern Indian Ocean. For instance, bacterial

* Supported by the China Ocean Mineral Resources R&D Association (Nos. DY135-B2-11, DY135-E2-4), the National Natural Science Foundation of China (No. 42076165), the Natural Science Foundation of Shandong Province (No. ZR2018MD017), the National Key Research and Development Program (No. 2016YFC1402301), and the Fundamental Research Funds for the Central Universities (No. 201822009)
** Corresponding authors: czs@fio.org.cn; mtbao@ouc.edu.cn
# Shujun LI and Zhisong CUI contributed equally to this work and should be regarded as co-first authors.

distribution in the deep-sea sediments of the Central Indian Ridge and the equator region of the Indian Ocean have been investigated (Hoek et al., 2003; Khandeparker et al., 2014). Qian et al. (2018) characterized the composition of bacterial and archaeal communities from rare earth elements-rich sediments at a depth of approximately 4 800 m in the Indian Ocean by Illumina high-throughput sequencing targeting 16S rRNA genes.

The mid-ocean ridges are unique ecosystems in terms of the structure of the benthic and pelagic communities they harbor, as well as the relatively high biomass of some ridges (Ingole and Koslow, 2005; Ramirez-Llodra et al., 2010). These ridges represent the current research hotspots (Ramirez-Llodra et al., 2010). Ninety-East Ridge (NER) is an earthquake-free ridge in the south-north direction along the line of 90°E in the Indian Ocean (Krishna et al., 1999). It is part of the mid-ocean ridge. In addition, NER is one of the most complicated regions exhibiting unique tectonic, topographic, bathymetric, and hydrographic features (Gao et al., 2021). These factors influence the distribution and ultimately the structuring of bacterial communities in water (Qian et al., 2018). However, it remains unclear how microbial communities respond differently to the changes in environmental conditions along the vertical gradient of various depths. Therefore, the study of the microbial community composition and biodiversity of the rarely-explored water column on NER in Indian Ocean can provide new insights into the structure and function of this unique bathypelagic ecosystem.

A water mass is a large body of water with relatively uniform physical, chemical, and biological characteristics and generally the same changing trends that exhibits significant differences from the surrounding seawater (Sverdrup et al., 1942; Yoshida et al., 1971). A water mass defines the diffusion boundary of the matter in it. Previous investigators used water masses to study the vertical microbial diversity of pelagic ecosystems. For instance, Lovejoy et al. (2006) analyzed the microbial eukaryote diversity of five different water masses in the Arctic Ocean using 18S rRNA gene clone library. In addition, another previous study characterized the taxonomic and functional community diversity of different water masses in the Southwestern Atlantic Ocean (SAO) (Junior et al., 2015). Compared with the microbial community diversity of the global ocean, the SAO harbored a significant portion of endemic gene diversity (Junior et al., 2015).

Improving our knowledge of the biodiversity of all microbial species is of great importance because ubiquitous and extensive interplay exists among different types of microbes so that they function as a whole to participate in important biogeochemical processes. However, almost all studies to date have only investigated a specific category of microorganisms rather than the whole microbial community, including bacteria, archaea, and fungi. For instance, Li et al. (2019a) assessed the depth-related distribution pattern of fungal communities along the water columns from the epi- to abyss-opelagic zones of the Western Pacific Ocean using internal transcribed spacer 2 (ITS2) metabarcoding. In addition, a previous study presented the first "snapshot" on biodiversity and spatial distribution of the bacteria in water columns in the Eastern Indian Ocean. This study suggested a more pronounced stratified distribution pattern with a detailed description of the bacterial community structure by pyrosequencing (Wang et al., 2016).

In view of the internal homogeneity of the water mass, we proposed the hypothesis that distinct microbial assemblage (including bacteria, archaea, and fungi) existed in different water masses on NER, and the microbial community structures were mainly controlled by the corresponding environmental factors of the water masses. In the present study, we first divided the water column samples from NER into five water masses according to the temperature-salinity curves (*T*-*S* curves). Then, we used high-throughput amplicon sequencing approach and bioinformatics to present a full and comparative description of the microbial community structure and biodiversity on NER, including bacteria, archaea, and fungi.

2 MATERIAL AND METHOD

2.1 Sampling and demarcation of water masses by *T*-*S* curves

Seawater was sampled with a CTD rosette (Seabird 911, SeaBird Electronics, Bellevue, Washington, USA) at 12 stations on NER (Fig.1a) from Dec. 2018 to Jan. 2019. Five samples were taken at depths ranging from 5 m to 5 000 m at each station. After sampling, the filtration has been done with a filter bowl (PALL, EastHills, NY, USA) and a diaphragm pump (Jinteng, Tianjin, China) on board. For epipelagic waters (depth <1 000 m), 2 L of seawater was filtered through a 0.22-μm pore-size membrane (Whatman, 47-mm diameter) at -0.08 MPa to collect

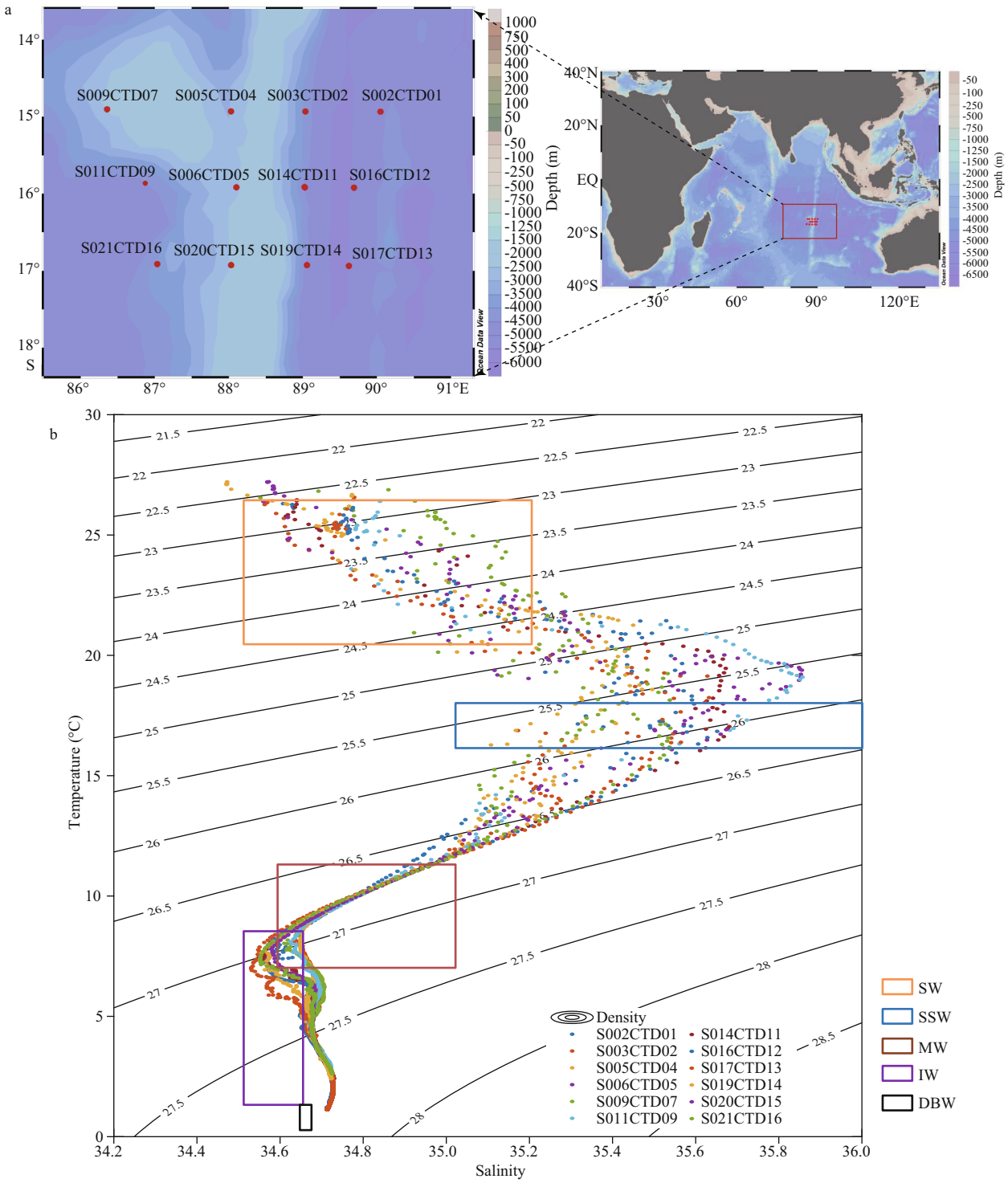

Fig.1 Investigation sites and different water masses on NER

a. the geographic locations of 12 sampling stations on NER. The red solid circles represent the investigation sites in Southern Indian Ocean; b. the presence of five different water masses on NER suggested by the *T-S* curves derived from the data of 12 CTD stations. The *X*-axis indicates salinity. The *Y*-axis indicates temperature (°C). The value on the isolines represents density of seawater (kg/m³), e.g., 27 represents 1 027 kg/m³ (the value +1 000). Different colored dots represent different stations. SW represents the water mass of surface water; SSW represents the water mass of subsurface water; MW represents the water mass of mode water; IW represents the water mass of intermediate water; DBW represents the water mass of deep water and bottom water.

microbial biomass. For bathypelagic waters (depth >1 000 m), 10 L of water was pretreated by the same method. Then, the membranes with biomass were kept at -80 °C on board prior to DNA extraction.

T-S curves were generated from the physical oceanographic data of these 12 stations using Matlab

Table 1 Five water masses on NER and their physical oceanographic features

Water masses on NER	Acronym	Physical oceanographic features				Number of samples	Brief description
		Temperature (°C)	Salinity	Density (kg/m^3)	Depth (m)		
Surface water	SW	20.0–27.0	34.4–35.2	1 024.5	<100	37	Trophic Indian Ocean surface water, broad range of temperature and salinity
Subsurface water	SSW	16.0–18.0	35.0–35.8	1 025.5	100–300	11	Relatively broad range of salinity
Mode water	MW	7.0–11.0	34.6–35.0	1 026.5–1 027.0	400–800	2	Liner relationship between temperature and salinity
Intermediate water	IW	3.0–9.0	34.5–34.65	1 027.0–1 027.5	800–1 500	2	Controlled by Antarctic intermediate water (AIW) transporting northward
Deep water and bottom water	DBW	1.0–3.0	34.65–34.70	1 027.5–1 027.75	>1 500	8	The variation of temperature and salinity is insignificant

(version R2010a) immediately after sampling. The profile of the *T-S* curves indicated the presence of five different water masses (Fig.1b; Table 1). Accordingly, these 60 water samples were sorted into 5 water masses in order to analyze the vertical distribution of the microbial community (Hanawa and Talley, 2001; Yao et al., 2017).

2.2 Physical and chemical parameters

At each sampling station, a CTD profiler was deployed to record temperature, depth, salinity, pH, and dissolved oxygen profiles. Samples for the analysis of dissolved nutrients (nitrate, phosphate, and silicate) were filtered onto Whatman GF/F fiberglass filters, and stored at -20 °C. The chemical parameters of seawaters with depth less than or equal to 500 m were analyzed as described by Park (1969), while those of seawaters with depth greater than 500 m were downloaded from GLODAPv2 data (Key et al., 2015; Lauvset et al., 2016; Olsen et al., 2016).

2.3 Total genomic DNA extraction

Total genomic DNA was extracted from the membrane samples described in Section 2.1 with Fast DNA SPIN extraction kits (MP Biomedicals, Santa Ana, CA, USA). Afterwards, DNA concentration was measured by NanoDrop ND-1000 spectrophotometer (Thermo Fisher Scientific, Waltham, MA, USA). The DNA molecular size was estimated by 0.8% (w/v) agarose gel electrophoresis. Then, the extracted DNA samples were stored at -80 °C.

2.4 High-throughput amplicon sequencing and data analysis

The V3-V4 region of the 16S rRNA gene was amplified from the bacterial DNA by PCR using the forward primer 5′-ACTCCTACGGGAGGCAGCA-3′ and the reverse primer 5′-GGACTACHVGGGTWTCTAAT-3′ (Claesson et al., 2009). The V4–V5 region of the 16S rRNA gene was amplified from the archaeal DNA by PCR using the forward primer 5′-TGYCAGCCGCCGCGGTAA-3′ and the reverse primer 5′-YCCGGCGTTGAVTCCAATT-3′ (Pires et al., 2012). The ITS1 region was amplified from the fungal DNA by PCR using the forward primer 5′-GGAAGTAAAAGTCGTAACAAGG-3′ and the reverse primer 5′-GCTGCGTTCTTCATCGATGC-3′ (White et al., 1990). Sample-specific 7-bp barcodes were incorporated into the primers for multiplex sequencing. The PCR components contained 5 μL of buffer (5×), 0.25 μL of Fast Pfu DNA Polymerase (5 U/μL), 2 μL (2.5 mmol/L) of dNTPs, 1 μL (10 μmol/L) of each forward and reverse primer, 1 μL of DNA Template, and 14.75 μL of ddH_2O. Thermal cycling consisted of initial denaturation at 98 °C for 5 min, followed by 25 cycles consisting of denaturation at 98 °C for 30 s, annealing at 53 °C for 30 s, and extension at 72 °C for 45 s, with a final extension of 5 min at 72 °C. PCR amplicons were purified with Vazyme VAHTSTM DNA Clean Beads (Vazyme, Nanjing, China), and quantified using the Quant-iT PicoGreen dsDNA Assay Kit (Invitrogen, Carlsbad, CA, USA). After the individual quantification step, amplicons were pooled in equal amounts. Then, the sequencing library was prepared using TruSeq Nano DNA LT Library Prep Kit from Illumina (San Diego, California, USA). Finally, pair-end 2×250 bp sequencing was performed using the Illumina NovaSeq platform with NovaSeq 6000 SP Reagent Kit (500 cycles) at Shanghai Personal Biotechnology Co., Ltd. (Shanghai, China).

QIIME 2 (Bokulich et al., 2018; Bolyen et al., 2019) was used to do downstream analysis of raw sequence data generated by PE250. Briefly, raw sequence data were demultiplexed using the demux plugin followed by primers cutting with the cutadapt

Table 2 Alpha diversity indices of microbial communities in different water masses on NER

Microbial taxa	Water mass	Chao1	Simpson	Shannon	Pielou's evenness	Observed species	Good's coverage
Bacteria	SW	967	0.97	7.06	0.72	884	0.995
	SSW	1 384	0.99	8.21	0.80	1 280	0.993
	MW	1 602	0.99	8.41	0.80	1 489	0.992
	IW	1 527	0.99	8.25	0.79	1 419	0.992
	DBW	1 068	0.97	7.04	0.71	985	0.994
Archaea	SW	316	0.91	4.89	0.62	290	0.999
	SSW	1 105	0.98	7.57	0.76	1 015	0.996
	MW	1 053	0.97	7.22	0.73	1 001	0.997
	IW	701	0.92	6.17	0.66	663	0.998
	DBW	509	0.96	6.39	0.72	479	0.999
Fungi	SW	297	0.78	4.20	0.51	295	1.000
	SSW	357	0.84	4.90	0.58	356	1.000
	MW	176	0.42	1.90	0.26	175	1.000
	IW	226	0.40	1.95	0.25	225	1.000
	DBW	232	0.83	4.42	0.56	232	1.000

SW: water mass of surface water; SSW: water mass of subsurface water; MW: water mass of mode water; IW: water mass of intermediate water; DBW represents the water mass of deep water and bottom water.

plugin (Martin, 2011). Sequences were then quality filtered, denoised, merged, and chimera removed using the DADA2 plugin (Callahan et al., 2016) (Supplementary Tables S1–S3). Non-singleton amplicon sequence variants (ASVs) were aligned with mafft (Kazutaka et al., 2002) and used to construct a phylogeny with fasttree2 (Price et al., 2009). Bacterial samples were rarefied to 26 600 sequences per sample. Archaeal samples were rarefied to 34 800 sequences per sample. Fungal samples were rarefied to 44 920 sequences per sample. Alpha-diversity metrics, including Chao1 (Chao, 1984), Observed species, Shannon (Shannon, 1948), Simpson (Simpson, 1949), Pielou's evenness (Pielou, 1966), and Good's coverage (Good, 1953), and beta diversity metrics (Jaccard distance) were estimated using the diversity plugin. Taxonomy was assigned to ASVs using the classify-sklearn naïve Bayes taxonomy classifier in feature-classifier plugin (Bokulich et al., 2018) against the SILVA Release 132 (bacteria and archaea) /UNITE Release 8.0 (fungi) Database (Kõljalg et al., 2013).

2.5 Statistic analysis

Sequence data analyses were mainly performed using QIIME2 and R packages (v3.2.0). We used non-metric multidimensional scaling (NMDS) to describe the distribution characteristics of samples with Jaccard distance. We also used an analysis of similarities (ANOSIM) to compare microbial community structures among different water masses. Redundancy analysis (RDA) was used to test the relationships between environmental parameters and microbial communities to extract principal environmental factors influencing the microbial communities. The *P* value of the RDA was obtained by Monte Carlo substitution test. A linear discriminant analysis effect size (LEfSe) (Segata et al., 2011) was carried out to determine indicator species in the microbial community.

3 RESULT AND DISCUSSION

3.1 Alpha diversity of microbial communities in different water masses on NER

The alpha diversity of microbial communities on NER was compared among water masses (Table 2). Good's coverage of microbial communities in each water mass was almost 1.000, indicating that the sequencing data was sufficient to reflect the microbial community diversity in the five water masses on NER.

From the perspective of species, bacteria exhibited the highest richness (Chao1: 967–1 602; observed species: 884–1 489), followed by archaea (Chao1: 316–1 105; observed species: 290–1 015) (Table 2). Fungi exhibited the lowest richness (Chao1: 176–357; observed species: 175–356). Similarly, bacteria exhibited the highest diversity (Shannon, 7.04–8.41;

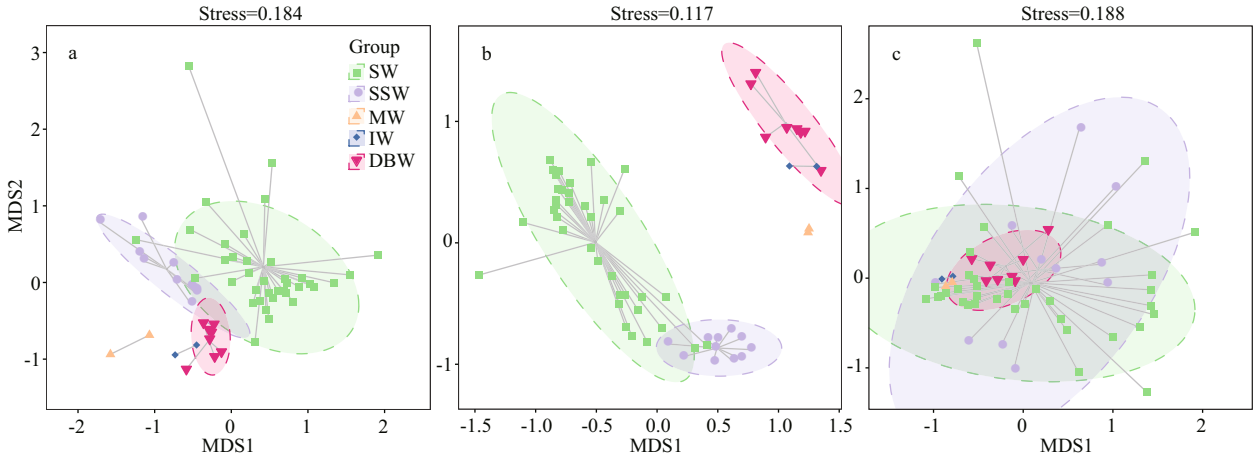

Fig.2 The dissimilarity of microbial community structure among the five water masses on NER by NMDS analysis

a. bacteria; b. archaea; c. fungi. Stress<0.2 indicates that the results of NMDS analysis are reliable. Each colored point represents the microbial community structure of a water sample on NER. The dotted line ellipse indicates 95% confidence, which means that 95 out of 100 samples in this sample set will fall into it. The center point of dotted line ellipse represents the mean value of all samples in each water mass. SW: water mass of surface water; SSW: water mass of subsurface water; MW: water mass of mode water; IW: water mass of intermediate water; DBW: water mass of deep water and bottom water.

Simpson, 0.97–0.99), followed by archaea (Shannon, 4.89–7.57; Simpson, 0.91–0.98). Fungi exhibited the lowest diversity (Shannon, 1.90–4.90; Simpson, 0.40–0.84). Bacteria also exhibited the highest evenness (0.71–0.80), followed by archaea (0.62–0.76). Fungi exhibited the lowest evenness (0.25–0.58). Furthermore, a dissimilarity analysis based on one-way analysis of variance (ANOVA) showed that microbial alpha diversity in the water column on NER was significantly different among bacteria, archaea, and fungi (Supplementary Table S4) (P<0.01). In brief, the alpha diversity of bacteria in the water column on NER was highest, followed by that of archaea. In contrast, fungi exhibited the lowest alpha diversity.

3.2 Beta diversity of microbial communities in different water masses on NER

NMDS analysis was conducted to demonstrate the difference among the microbial community structures in each water mass (Fig.2). The result of NMDS analysis was relatively reliable for bacteria, archaea, and fungi (stress value <0.2) (Legendre and Legendre, 1998).

The distance between two points on the plot indicated the discrepancy of the microbial community structures between the corresponding two water samples. With respect to bacterial and archaeal community structure, the samples derived from the same water mass formed a distinct and separate cluster on the plot. The discrepancy within the samples from the same water mass was lower than those of the samples derived from different water masses. In contrast, the fungal community structure within the samples of the same water mass could exhibit even higher discrepancy than that of the water samples derived from different water masses. In addition, we performed an analysis of similarities (ANOSIM) of microbial community structure among the five water masses on NER (Supplementary Table S5). Both the bacterial and archaeal community structures exhibited significant differences among different water masses on NER (P<0.01). In contrast, the fungal community structures exhibited no significant differences among different water masses on NER (P>0.05).

In the open oceans, dispersal of bacteria and archaea is relatively passive (Winter et al., 2013), suggesting that the movement of prokaryotes might be constrained by the interface of water mass. Different water masses exhibit distinct physical oceanographic and chemical features, which are optimum for microbes with the specific traits to grow. Therefore, distinct prokaryotic community structures were stratified in corresponding water masses on NER, especially that of archaea (Fig.2; Supplementary Table S5). In another previous study, Celussi et al. (2010) analyzed bacterial community structure of five Ross Sea water masses using denaturing gradient gel electrophoresis. The results showed that different water masses on Ross Sea also harbored diverse bacterial communities.

In contrast, fungal species were eurybathic in different water masses on NER, which was consistent with previous findings on the distribution pattern of fungal species in the deep sea (Li et al., 2019a).

Moreover, Wang et al. (2019) assessed the diversity and distribution of fungal communities from the Mariana Trench with a depth range of 1 000–4 000 m using Illumina Hiseq sequencing. The results indicated that there were many fungal taxa resources in the seawater of the Mariana Trench, and most of the same fungal species were found at various depths.

In short, the changing environmental factors across water masses might play a key role in the formation and stabilization of prokaryotic microbial communities, but exerted limited impact on fungal community distribution.

3.3 Microbial community structure in different water masses on NER

Each water mass on NER is distinct with respect to the physical oceanographic features (Table 1), which favor or inhibit the growth of specific microbes living in the water masses (Guo et al., 2018). Therefore, different water masses usually harbor significantly different microbial communities. We looked into the species composition of the microbial communities in the five water masses on NER by sequencing and alignment of 16S rRNA and ITS1 genes (Fig.3).

From the perspective of bacterial species composition at the level of phylum (Fig.3a), Proteobacteria was predominant among the bacterial ASVs (>59.0%), which was consistent with previous findings on oceanic bacterial diversity (Medina-Silva et al., 2018). Actinobacteria, Bacteroidetes, Chloroflexi, Deinococcus-Thermus, Acidobacteria, and Marinimicrobia (SAR406 clade) were backbone members across the five water masses on NER, though the relative abundance of them varied from water mass to water mass. More specifically, Cyanobacteria are capable of performing photosynthesis and nitrogen fixation in the presence of light and oxygen (Herrero et al., 2001). Therefore, Cyanobacteria were the more abundant member in SW (9.7%) with available sunlight. The salinity range in SSW is relatively broader. Chloroflexi and Acidobacteria exhibit adaptability to wide range of changing salinity. Hence, these two phyla prevailed in SSW (Zhao et al., 2020). We found abundant Chloroflexi and Marinimicrobia (SAR406 clade) in MW and IW, because these two phyla mainly exist in the transition phase from the euphotic to the aphotic layers (Korlević et al., 2015). In addition, members of Actinobacteria thrive in DBW, because they adapt more easily to hostile environmental conditions in the deep ocean (Sayed et al., 2020). Each water mass harbors several dominant bacterial phyla that adapt best to the corresponding environmental conditions of the water mass.

Regarding archaea, Euryarchaeota and Thaumarchaeota were the two predominant phyla in each water mass (Fig.3b). They have been detected in all the oceans of the world, and are ubiquitous from surface waters to the deep sea (Pereira et al., 2019). We found that Euryarchaeota was most predominant in SW, while its relative abundance dropped dramatically with increasing depth (from 80.6% in SW to 32.1% in the other four water masses). In contrast, the abundance of Thaumarchaeota was relatively lower in SW than in the rest of the water masses, but it surpassed Euryarchaeota as the most dominant archaeal phylum with increasing depth (from 18.5% in SW to 67.8% in the other four water masses). In addition, other phyla of low relative abundance (<0.1%) were also present in the water masses (Supplementary Table S6). In summary, our study reinforced previous findings by high-throughput amplicon sequencing that Euryarchaeota and Thaumarchaeota represented the majority of the sequences in the archaeal communities from extensive regions of the world's oceans, including the Pacific Ocean, the South China Sea, and Jeju Island (Choi et al., 2016; Xia et al., 2017; Li et al., 2019b).

Regarding fungi, Ascomycota (41.1%–95.1%) was the single dominant phylum across the five water masses, followed by Basidiomycota (0.6%–5.4%) (Fig.3c). Moreover, there were also several phyla exhibiting low relative abundance (<0.07%) in the water masses (Supplementary Table S7). This profile at the phylum level was identical to that of the Central Indian Ocean Basin, which was described in the first report on culture-independent diversity of fungi from the Indian Ocean (Singh et al., 2011). Our results reinforced previous findings that Ascomycota is the largest and most widespread phylum of fungi in deepsea environments (Nagano and Nagahama, 2012; Xu et al., 2014; Li et al., 2019a).

From the perspective of bacterial species composition at the level of genus (Fig.3d), *Candidatus Actinomarina* was the dominant genus in SW. Sva0996 marine group, also an actinobacterial taxa, was predominant in MW. Actinobacteria can assimilate phytoplankton-derived dissolved protein and are involved in the cycling of dissolved organic nitrogen in the ocean (Orsi et al., 2016). Three bacterial genera (*Thermus*, *Halomonas*, and *Leeuwenhoekiella*) were predominant in IW. Strains of *Leeuwenhoekiella* spp. are pressure-resistant, and

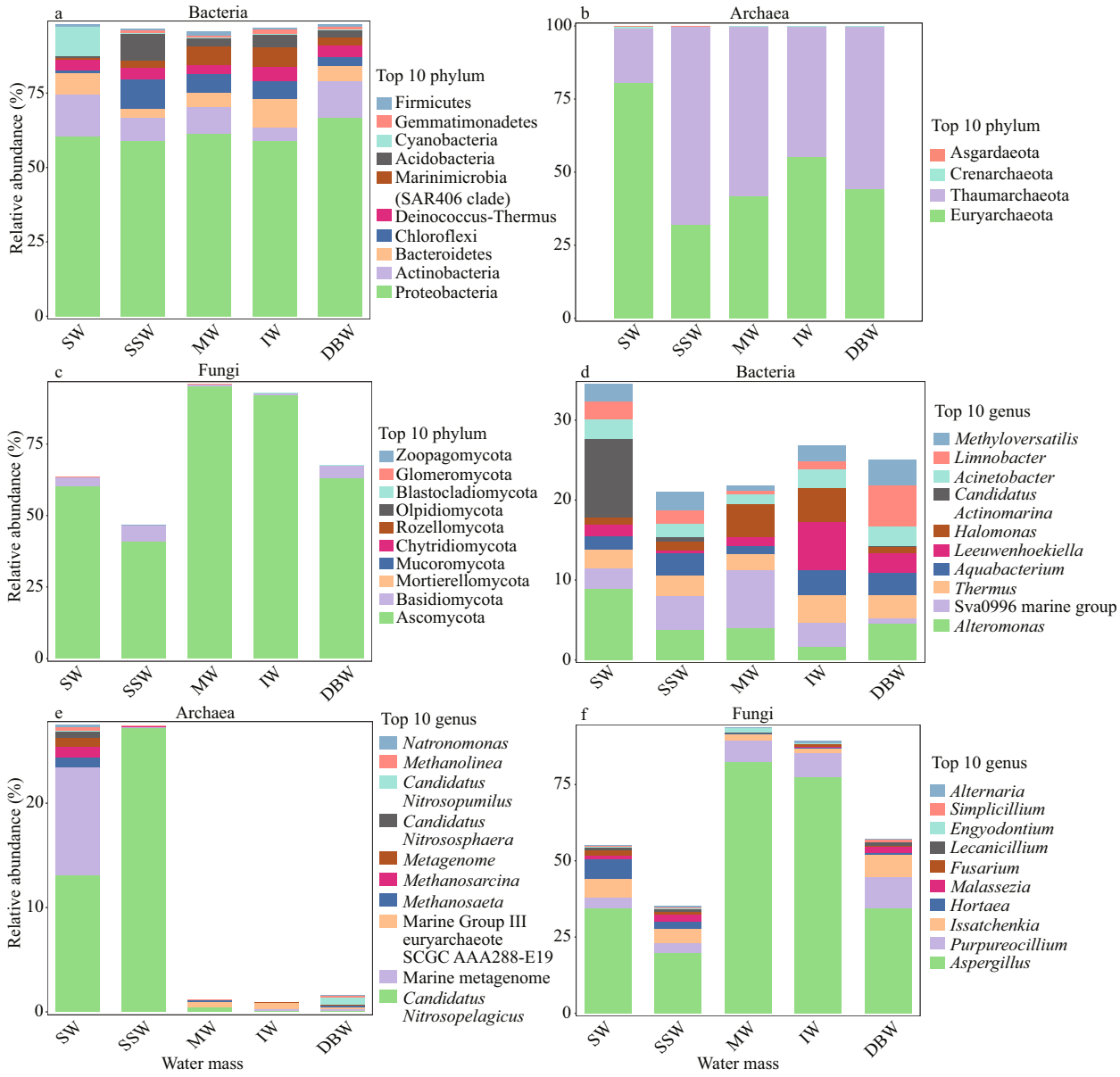

Fig.3 Relative abundance of the top 10 dominant ASVs in the five water masses at the level of phylum and genus

a. bacterial ASVs at the level of phylum; b. archaeal ASVs at the level of phylum; c. fungal ASVs at the level of phylum; d. bacterial ASVs at the level of genus; e. archaeal ASVs at the level of genus; f. fungal ASVs at the level of genus. The size of the bar indicates the relative abundance of the ASVs. SW: water mass of surface water; SSW: water mass of subsurface water; MW: water mass of mode water; IW: water mass of intermediate water; DBW: water mass of deep water and bottom water.

have been isolated and characterized from the deep sea environment many times (Liu et al., 2016). *Limnobacter* and *Methyloversatilis* were the dominant genera in the DBW. *Limnobacter* is the dominant species of DBW owing to its psychrotolerant features (Maity et al., 2012).

It was readily apparent that the relative abundance of archaeal genera in three water masses (MW, IW, and DBW) was surprisingly low (Fig.3e). This profile was generated for two reasons: 1) most archaeal ASVs in MW, IW, and DBW could not be identified at the genus level, and 2) only the identified archaeal genera were represented in the bar graph. Therefore, most unidentified members were not represented even though they might be abundant in the corresponding water mass. *Candidatus Nitrosopelagicus* was the dominant archaeal member in SW. Similarly, *Ca. Nitrosopelagicus* was the single dominant archaeal member in SSW. In addition, Marine Group III euryarchaeote SCGC AAA288-E19 was the dominant archaeal member in MW and IW. *Ca. Nitrosopumilus* was dominant in the DBW. *Ca. Nitrosopelagicus* and

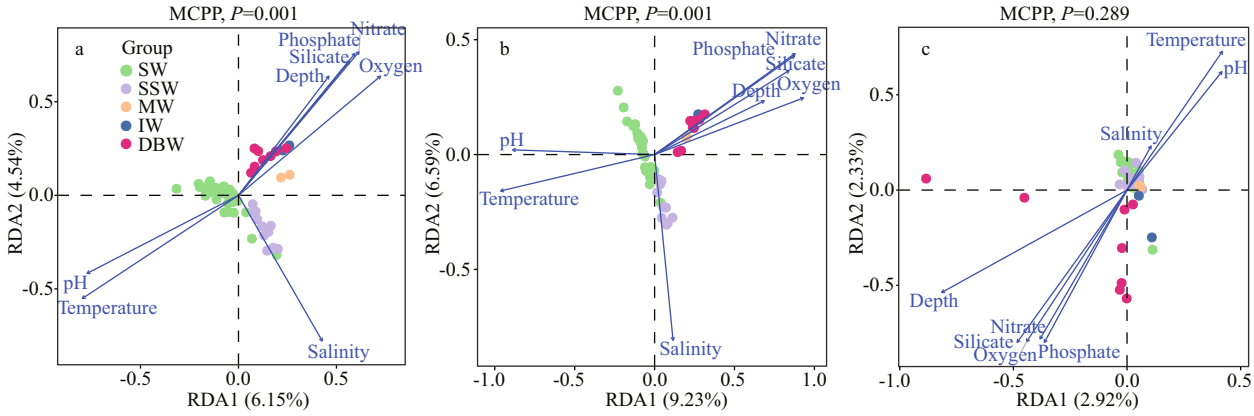

Fig.4 Redundancy analysis of the effect of environmental factors on microbial community structure in different water masses on NER

a. bacteria; b. archaea; c. fungi. Each colored point represents the microbial community structure of a water sample. Points of different colors indicate different water masses. Arrows represent different influencing environmental factors. The longer the arrow is, the greater the influence of this factor on the microbiome will be. SW: water mass of surface water; SSW: water mass of subsurface water; MW: water mass of mode water; IW: water mass of intermediate water; DBW: water mass of deep water and bottom water.

Ca. *Nitrosopumilus* are both ammonia-oxidizing archaea (Park et al., 2012; Carini et al., 2018). The identified lineages of this phylum are known to be ammonia oxidizers that might play a significant role in natural biogeochemical cycles such as nitrogen cycling (Pester et al., 2011; Hatzenpichler, 2012).

The top 10 most abundant fungal genera made up 66.15% of the fungal communities in the water column on NER (Fig.3f). This proportion was much higher than that of bacteria and archaea, indicating a less complex fungal community structure. The relative abundance of *Aspergillus* was the highest across the five water masses, especially in MW and IW (>78%). The next predominant genera were *Purpureocillium* and *Issatchenkia*. *Aspergillus* was among the most common fungal genera in deep-sea ecosystems (Nagano and Nagahama, 2012). The class Archaeorhizomycetes, which includes most characterized *Aspergillus* species, exhibits its broad distribution across diverse ecosystems and its high species diversity within sites (Rosling et al., 2013). Rosling et al. (2011) formally described it as comprising hundreds of cryptically reproducing filamentous species that do not form recognizable mycorrhizal structures and have a saprotrophic lifestyle.

3.4 Environmental factors affecting the structure of microbial communities in the different water masses on NER

The physical and chemical parameters of 60 seawater samples derived from NER were summarized in Table 1. Then, RDA was performed between the structure of microbial communities in water masses on NER and the corresponding environmental parameters to explore their correlations (Fig.4). It can be easily seen that environmental factors exerted significant impacts on the structure of bacterial and archaeal communities in each water mass (P=0.001) (Fig.4a–b). On the contrary, the same environmental factors exerted insignificant impacts on the structure of fungal communities in each water mass (P>0.05) (Fig.4c). In order to further determine the variables which significantly influence microbial community structure, a forward selection procedure (Uraibi et al., 2017) was performed (Supplementary Table S8). The results showed that environmental factors including temperature, salinity, depth, and nitrate, phosphate, and silicate content exhibited a significant influence on bacterial and archaeal communities (P<0.05). In contrast, only temperature and nitrate exhibited significant effects on the fungal community (P<0.05).

The bacterial communities in SW were significantly influenced by temperature (Fig.4a; P=0.001) (Supplementary Table S8; P<0.05). At the global scale, positive correlations between bacterial richness and sea-surface temperature have been observed (Pommier et al., 2007; Fuhrman et al., 2015). Sunagawa et al. (2015) demonstrated that vertical stratification of epipelagic and mesopelagic bacterial communities was mostly driven by temperature using metagenomic data from 68 different sites across different oceans. However, the SSW bacterial community was strongly influenced by salinity (Fig.4a; P=0.001) (Supplementary Table S8; P<0.05). The salinity in SSW changed in very broad range, so

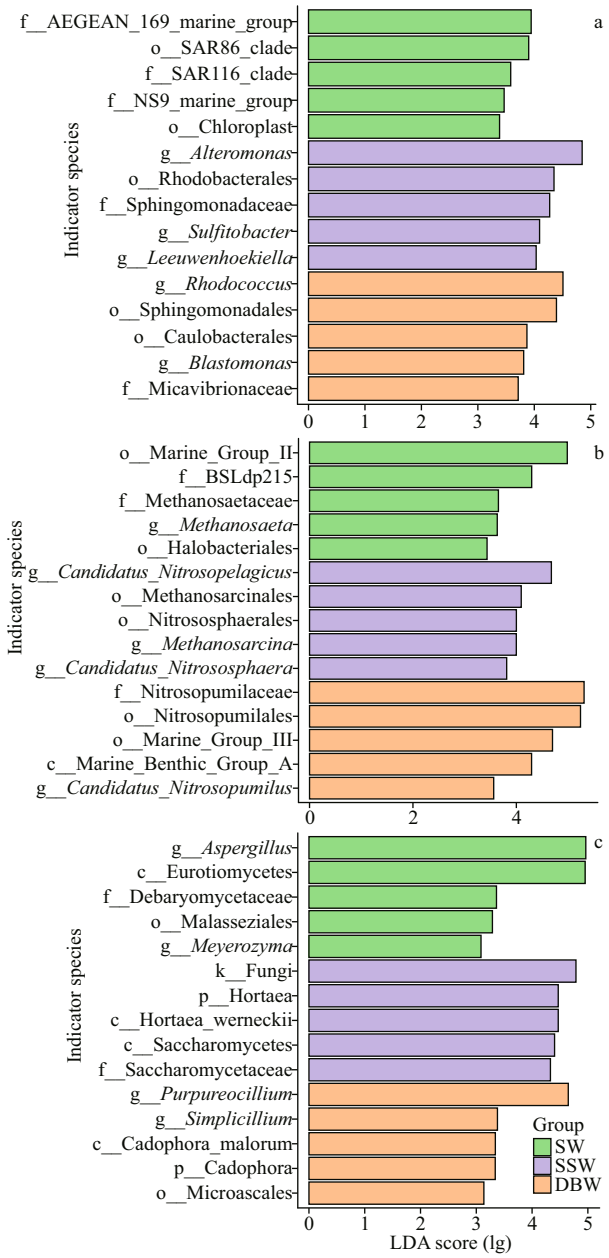

Fig.5 The top five indicator species in different water masses on NER by LEfSe analysis

a. bacteria; b. archaea; c. fungi. A significance alpha of 0.05 and an effect size threshold of 2 were used for all biomarkers evaluated. The indicator species in different water masses are listed on the left. The linear discriminant analysis (LDA) score is on the bottom. SW: water mass of surface water; SSW: water mass of subsurface water; DBW: water mass of deep water and bottom water. LEfSe analysis results of MW and IW are not available due to insufficient samples from these two water masses.

that only microbes capable of efficiently adapting to the shifting salinity could survive (Kuchi and Khandeparker, 2020). The bacterial communities in MW, IW, and DBW exhibited stronger relationships with combined parameters, including depth and nitrate, phosphate, and silicate content (Fig.4a; P=0.001) (Supplementary Table S8; P<0.05). Since temperature and salinity are relatively constant in deeper water masses, including MW, IW, and DBW, the bacterial community is more susceptible to the changing parameters including pressure (depth) and nutrients (Gao et al., 2021). Consequently, the environmental factors (temperature, salinity, depth, and nitrate, phosphate, and silicate content) exerted significant impacts on bacterial communities in various water masses.

The environmental parameters affecting the archaeal community structure in each water mass were identical to those of bacteria (Fig.4a–b; P=0.001). We speculated that prokaryotic species shared similar adaptation mechanisms to change in the environment in water masses on NER (Gao et al., 2021).

The RDA results clearly demonstrated that single or multiple combined environmental factors altered the prokaryotic community structures in different water masses on NER. Here, temperature was a key environmental variable affecting the prokaryotic communities in SW, salinity was a key environmental variable affecting the prokaryotic communities in SSW, and combined environmental parameters (including depth and nitrate, phosphate, and silicate content) played a pivotal role in affecting the prokaryotic communities in deeper water masses, including MW, IW, and DBW.

3.5 Indicator species of the microbial communities in different water masses on NER

The standardized heatmap presents the top 30 most abundant microbial genera in each water mass on NER (Supplementary Fig.S1). Remarkably, each water mass was distinguished by a phylogenetically close cluster of genera, the abundance of which was higher than that of the rest water masses. In contrast, the genera of high abundance derived from different water masses were phylogenetically distant from each other. Therefore, these results suggested the presence of signature microbial taxa in each water mass on NER. Furthermore, LEfSe and cladogram analyses were performed to determine the indicator species of bacteria, archaea, and fungi in SW, SSW, and DBW, respectively (Fig.5, Supplementary Fig.S2).

With respect to bacteria, the AEGEAN 169 marine group, SAR116 clade, and NS9 marine group were the main indicator species in SW (Fig.5a). *Alteromonas*, *Leeuwenhoekiella*, *Sulfitobacter*, and Sphingomonadaceae were the main indicator species in SSW. *Rhodococcus*, Micavibvionaceae, and

Blastomonas were the main indicator species in DBW. The indicator species of each water mass adapt well to the environmental conditions of the water mass in which they reside. For example, the AEGEAN 169 marine group exhibits a potentially interesting adaptation to high solar irradiance (Reintjes et al., 2019), the abundance of which is closely related to phytoplanktons (Yang et al., 2015). *Alteromonas* exhibits relatively strong tolerance to salinity, so it could adapt to the SSW environment (Qin et al., 2020). In addition, strains of *Rhodococcus* have been characterized as piezophiles (Picard and Daniel, 2013). Therefore, this genus could adapt to hostile deep-sea environments with high hydrostatic pressure (Hackbusch et al., 2020).

Among the archaea, BSLdp215 and Methanosaetaceae were the main indicator species in SW (Fig.5b). *Candidatus Nitrosopelagicus*, *Canidatus Nitrososphaera*, and *Methanosarcina* were the main indicator species in SSW. *Canidatus Nitrosopumilus* and Nitrosopumilaceae were the main indicator species in DBW. The archaeal indicator species in each water mass are also well-adapted to the physicochemical conditions of the corresponding water mass. For instance, *Candidatus Nitrosopelagicus* can grow chemolithoautotrophically by aerobically oxidizing ammonia to nitrite (Brochier-Armanet et al., 2008). Thus, aerobic ammonia oxidation appears to be an important pathway in nitrogen cycling in SSW. In addition, several studies have demonstrated that Nitrosopumilaceae are more frequently recovered from deep water (Wemheuer et al., 2019).

With respect to fungi, Debaryomycetaceae was the main indicator species in SW (Fig.5c). Saccharomycetaceae was the main indicator species in SSW. *Simpcicillium* and *Purpureocillium* were the main indicator species in DBW. Again, the fungal indicator species adapt well to the environmental conditions of each water mass, but there are fewer indicator species at the levels of family and genus.

In short, LEfSe and cladogram analyses further suggested that different water masses on NER harbor distinct microbial taxa that represent the biological features of the corresponding water mass to some extent. The indicator species dwelling in each water mass might be used as fingerprints to discriminate corresponding water masses on NER. Though further studies are needed to reinforce this assertion, the present study presented a potential method to identify oceanic water masses using microbiology.

4 CONCLUSION

In the present study, we sorted 60 pelagic water samples on NER into five water masses using featured *T-S* curves. The vertical stratification and diversity of microbial communities in each water mass were characterized. Bacteria exhibited the highest richness and diversity across the water masses on NER. RDA results suggested that environmental factors in the water masses might play a pivotal role in the formation and stability of the distinct prokaryotic community structure in each water mass. LEfSe analysis further revealed that each water mass harbored distinct indicator species. These indicator species might be used as potential signatures to identify the corresponding water masses on NER. These results substantially reinforced the biological nature of pelagic water masses from the perspective of microbiology. In conclusion, it is robust and feasible to study the vertical distribution, structure, and diversity of microorganisms in pelagic ecosystems based on water masses.

5 DATA AVAILABILITY STATEMENT

The NovaSeq FASTQ files and the identifier barcode files were deposited in the National Center for Biotechnology Information Sequence Read Archive (SRA) under BioProject Accession No. PRJNA655383 (https://www.ncbi.nlm.nih.gov/sra/PRJNA655383).

6 ACKNOWLEDGMENT

This is the Key Laboratory of Marine Chemistry Theory and Technology (Ocean University of China), Ministry of Education (MCTL) (Contribution No. 249).

References

Arrigo K R. 2005. Marine microorganisms and global nutrient cycles. *Nature*, **437**(7057): 349-355, https://doi.org/10.1038/nature04159.

Bokulich N A, Kaehler B D, Rideout J R, Dillon M, Bolyen E, Knight R, Huttley G A, Caporaso J G. 2018. Optimizing taxonomic classification of marker-gene amplicon sequences with QIIME 2's q2-feature-classifier plugin. *Microbiome*, **6**: 90. https://doi.org/10.1186/s40168-018-0470-z.

Bolyen E, Rideout J R, Dillon M R, Bokulich N A, Abnet C C, Al-Ghalith G A, Alexander H, Alm E J, Arumugam M, Asnicar F, Bai Y, Bisanz J E, Bittinger K, Brejnrod A, Brislawn C J, Brown C T, Callahan B J, Caraballo-

Rodríguez A M, Chase J, Cope E K, Da Silva R, Diener C, Dorrestein P C, Douglas G M, Durall D M, Duvallet C, Edwardson C F, Ernst M, Estaki M, Fouquier J, Gauglitz J M, Gibbons S M, Gibson D L, Gonzalez A, Gorlick K, Guo J R, Hillmann B, Holmes S, Holste H, Huttenhower C, Huttley G A, Janssen S, Jarmusch A K, Jiang L J, Kaehler B D, Kang K B, Keefe C R, Keim P, Kelley S T, Knights D, Koester I, Kosciolek T, Kreps J, Langille M G I, Lee J, Ley R, Liu Y X, Loftfield E, Lozupone C, Maher M, Marotz C, Martin B D, McDonald D, McIver L J, Melnik A V, Metcalf J L, Morgan S C, Morton J T, Naimey A T, Navas-Molina J A, Nothias L F, Orchanian S B, Pearson T, Peoples S L, Petras D, Preuss M L, Pruesse E, Rasmussen L B, Rivers A, Robeson M S II, Rosenthal P, Segata N, Shaffer M, Shiffer A, Sinha R, Song S J, Spear J R, Swafford A D, Thompson L R, Torres P J, Trinh P, Tripathi A, Turnbaugh P J, Ul-Hasan S, van der Hooft J J J, Vargas F, Vázquez-Baeza Y, Vogtmann E, von Hippel M, Walters W, Wan Y H, Wang M X, Warren J, Weber K C, Williamson C H D, Willis A D, Xu Z Z, Zaneveld J R, Zhang Y L, Zhu Q Y, Knight R, Caporaso J G. 2019. Reproducible, interactive, scalable and extensible microbiome data science using QIIME 2. *Nature Biotechnology*, **37**(8): 852-857, https://doi.org/10.1038/s41587-019-0209-9.

Brochier-Armanet C, Boussau B, Gribaldo S, Forterre P. 2008. Mesophilic crenarchaeota: proposal for a third archaeal phylum, the Thaumarchaeota. *Nature Reviews Microbiology*, **6**(3): 245-252, https://doi.org/10.1038/nrmicro1852.

Callahan B J, McMurdie P J, Rosen M J, Han A W, Johnson A J A, Holmes S P. 2016. DADA2: high-resolution sample inference from Illumina amplicon data. *Nature Methods*, **13**(7): 581-583, https://doi.org/10.1038/nmeth.3869.

Carini P, Dupont C L, Santoro A E. 2018. Patterns of thaumarchaeal gene expression in culture and diverse marine environments. *Environmental Microbiology*, **20**(6): 2112-2124, https://doi.org/10.1111/1462-2920.14107.

Celussi M, Bergamasco A, Cataletto B, Umani S F, Del Negro P. 2010. Water masses' bacterial community structure and microbial activities in the Ross Sea, Antarctica. *Antarctic Science*, **22**(4): 361-370, https://doi.org/10.1017/S0954102010000192.

Chao A. 1984. Nonparametric estimation of the number of classes in a population. *Scandinavian Journal of Statistics*, **11**(4): 265-270.

Choi H, Koh H W, Kim H, Chae J C, Park S J. 2016. Microbial community composition in the marine sediments of Jeju Island: next-generation sequencing surveys. *Journal of Microbiology and Biotechnology*, **26**(5): 883-890, https://doi.org/10.4014/jmb.1512.12036.

Claesson M J, O'Sullivan O, Wang Q, Nikkilä J, Marchesi J R, Smidt H, de Vos W M, Ross R P, O'Toole P W. 2009. Comparative analysis of pyrosequencing and a phylogenetic microarray for exploring microbial community structures in the human distal intestine. *PLoS One*, **4**(8): e6669, https://doi.org/10.1371/journal.pone.0006669.

Fuhrman J A, Cram J A, Needham D M. 2015. Marine microbial community dynamics and their ecological interpretation. *Nature Reviews Microbiology*, **13**(3): 133-146, https://doi.org/10.1038/nrmicro3417.

Gao P, Qu L Y, Du G X, Wei Q S, Zhang X L, Yang G. 2021. Bacterial and archaeal communities in deep sea waters near the Ninetyeast Ridge in Indian Ocean. *Journal of Oceanology and Limnology*, **39**(2): 582-597, https://doi.org/10.1007/s00343-020-9343-y.

Good I J. 1953. The population frequencies of species and the estimation of population parameters. *Biometrika*, **40**(3-4): 237-264, https://doi.org/10.2307/2333344.

Guo X P, Lu D P, Niu Z S, Feng J N, Chen Y R, Tou F Y, Liu M, Yang Y. 2018. Bacterial community structure in response to environmental impacts in the intertidal sediments along the Yangtze Estuary, China. *Marine Pollution Bulletin*, **126**: 141-149, https://doi.org/10.1016/j.marpolbul.2017.11.003.

Hackbusch S, Noirungsee N, Viamonte J, Sun X X, Bubenheim P, Kostka J E, Müller R, Liese A. 2020. Influence of pressure and dispersant on oil biodegradation by a newly isolated *Rhodococcus* strain from deep-sea sediments of the Gulf of Mexico. *Marine Pollution Bulletin*, **150**: 110683,https://doi.org/10.1016/j.marpolbul.2019.110683.

Hanawa K, Talley L D. 2001. Mode waters. *International Geophysics*, **77**: 373-386, https://doi.org/10.1016/S0074-6142(01)80129-7.

Hatzenpichler R. 2012. Diversity, physiology, and niche differentiation of ammonia-oxidizing archaea. *Applied and Environmental Microbiology*, **78**(21): 7501-7510, https://doi.org/10.1128/AEM.01960-12.

Herrero A, Muro-Pastor A M, Flores E. 2001. Nitrogen control in cyanobacteria. *Journal of Bacteriology*, **183**(2): 411-425, https://doi.org/10.1016/j.bmcl.2009.11.010.

Hoek J, Banta A, Hubler F, Reysenbach A L. 2003. Microbial diversity of a sulphide spire located in the Edmond deep-sea hydrothermal vent field on the Central Indian Ridge. *Geobiology*, **1**(2): 119-127, https://doi.org/10.1046/j.1472-4669.2003.00015.x.

Ingole B, Koslow J A. 2005. Deep-sea ecosystems of the Indian Ocean. *Indian Journal of Marine Sciences*, **34**(1): 27-34.

Junior N A, Meirelles P M, de Oliveira Santos E, Dutilh B, Silva G G Z, Paranhos R, Cabral A S, Rezende C, Iida T, de Moura R L, Kruger R H, Pereira R C, Valle R, Sawabe T, Thompson C, Thompson F. 2015. Microbial community diversity and physical-chemical features of the Southwestern Atlantic Ocean. *Archives of Microbiology*, **197**(2): 165-179, https://doi.org/10.1007/s00203-014-1035-6.

Kazutaka K, Kazuharu M, Ichi K K et al. 2002. MAFFT: a novel method for rapid multiple sequence alignment based on fast Fourier transform. *Nucleic Acids Research*, **30**(14): 3059-3066, https://doi.org/10.1093/nar/gkf436.

Key R M, Olsen A, van Heuven S, Lauvset S K, Velo A, Lin X H, Schirnick C, Kozyr A, Tanhua T, Hoppema M,

Jutterström S, Steinfeldt R, Jeansson E, Ishii M, Perez F F, Suzuki T. 2015. Global Ocean Data Analysis Project, Version 2 (GLODAPv2), ORNL/CDIAC-162, NDP-P093. Carbon Dioxide Information Analysis Center, Oak Ridge National Laboratory, US Department of Energy, Oak Ridge, Tennessee.

Khandeparker R, Meena R M, Deobagkar D. 2014. Bacterial diversity in deep-sea sediments from Afanasy Nikitin Seamount, equatorial Indian Ocean. *Geomicrobiology Journal*, **31**(10): 942-949, https://doi.org/10.1080/01490451.2014.918214.

Kõljalg U, Nilsson R H, Abarenkov K, Tedersoo L, Taylor A F S, Bahram M, Bates S T, Bruns T D, Bengtsson-Palme J, Callaghan T M, Douglas B, Drenkhan T, Eberhardt U, Dueñas M, Grebenc T, Griffith G W, Hartmann M, Kirk P M, Kohout P, Larsson E, Lindahl B D, Lücking R, Martín M P, Matheny P B, Nguyen N H, Niskanen T, Oja J, Peay K G, Peintner U, Peterson M, Põldmaa K, Saag L, Saar I, Schüßler A, Scott J A, Senés C, Smith M E, Suija A, Taylor D L, Telleria M T, Weiss M, Larsson K H. 2013. Towards a unified paradigm for sequence-based identification of fungi. *Molecular Ecology*, **22**(21): 5271-5277, https://doi.org/10.1111/mec.12481.

Korlević M, Ristova P P, Garić R, Amann R, Orlić S. 2015. Bacterial diversity in the South Adriatic Sea during a strong, deep winter convection year. *Applied and Environmental Microbiology*, **81**(5): 1715-1726, https://doi.org/10.1128/AEM.03410-14.

Krishna K S, Rao D G, Raju L V S, Chaubey A K, Shcherbakov V S, Pilipenko A I, Murthy I V R. 1999. Paleocene on-spreading-axis hotspot volcanism along the Ninetyeast Ridge: an interaction between the Kerguelen hotspot and the Wharton spreading center. *Journal of Earth System Science*, **108**(4): 255-267, https://doi.org/10.1007/BF02840503.

Kuchi N, Khandeparker L. 2020. Influence of salinity stress on bacterial diversity from a marine bioinvasion perspective: evaluation through microcosm experiments. *Current Science*, **119**(3): 507-525, https://doi.org/10.18520/cs/v119/i3/507-525.

Lauvset S K, Key R M, Olsen A, van Heuven S, Velo A, Lin X H, Schirnick C, Kozyr A, Tanhua T, Hoppema M, Jutterström S, Steinfeldt R, Jeansson E, Ishii M, Perez F F, Suzuki T, Watelet S. 2016. A new global interior ocean mapped climatology: the 1°×1° GLODAP version 2. *Earth System Science Data*, **8**(2): 325-340, https://doi.org/10.5194/essd-8-325-2016.

Legendre P, Legendre L. 1998. Numerical Ecology. 2nd edn. Elsevier, Amsterdam.

Li W, Wang M M, Burgaud G, Yu H M, Cai L. 2019a. Fungal community composition and potential depth-related driving factors impacting distribution pattern and trophic modes from epi- to abyssopelagic zones of the western Pacific Ocean. *Microbial Ecology*, **78**(4): 820-831, https://doi.org/10.1007/s00248-019-01374-y.

Li Y T, Zhu X Y, Zhang W M, Zhu D C, Zhou X J, Zhang L K. 2019b. Archaeal communities in the deep-sea sediments of the South China Sea revealed by Illumina high-throughput sequencing. *Annals of Microbiology*, **69**(8): 839-848, https://doi.org/10.1007/s13213-019-01477-4.

Liu Q F, Li J T, Wei B B, Zhang X Y, Zhang L, Zhang Y Z, Fang J S. 2016. *Leeuwenhoekiella nanhaiensis* sp. nov., isolated from deep-sea water. *International Journal of Systematic and Evolutionary Microbiology*, **66**(3): 1352-1357, https://doi.org/10.1099/ijsem.0.000883.

Lovejoy C, Massana R, Pedrós-Alió C. 2006. Diversity and distribution of marine microbial eukaryotes in the Arctic Ocean and adjacent seas. *Applied and Environmental Microbiology*, **72**(5): 3085-3095, https://doi.org/10.1128/AEM.72.5.3085-3095.2006.

Maity J P, Chen C Y, Nath B, Bundschuh J, Bhattacharya P. 2012. Geothermal arsenic in Taiwan: geochemistry and microbial diversity. *In*: Ng J C, Noller B N, Naidu R, Bundschuh J, Bhattacharya P eds. Understanding the Geological and Medical Interface of Arsenic. Taylor & Francis Group, London. p.483-485.

Martin M. 2011. Cutadapt removes adapter sequences from high-throughput sequencing reads. *EMBnet Journal*, **17**(1): 10-12, https://doi.org/10.14806/ej.17.1.200.

Medina-Silva R, De Oliveira R R, Pivel M A G, Borges L G A, Simão T L L, Pereira L M, Trindade F J, Augustin A H, Valdez F P, Eizirik E, Utz L R P, Groposo C, Miller D J, Viana A R, Ketzer J M M, Giongo A. 2018. Microbial diversity from chlorophyll maximum, oxygen minimum and bottom zones in the southwestern Atlantic Ocean. *Journal of Marine Systems*, **178**: 52-61, https://doi.org/10.1016/j.jmarsys.2017.10.008.

Nagano Y, Nagahama T. 2012. Fungal diversity in deep-sea extreme environments. *Fungal Ecology*, **5**(4): 463-471, https://doi.org/10.1016/j.funeco.2012.01.004.

Olsen A, Key R M, van Heuven S, Lauvset S K, Velo A, Lin X H, Schirnick C, Kozyr A, Tanhua T, Hoppema M, Jutterström S, Steinfeldt R, Jeansson E, Ishii M, Pérez F F, Suzuki T. 2016. The global ocean data analysis project version 2 (GLODAPv2) — an internally consistent data product for the world ocean. *Earth System Science Data*, **8**(2): 297-323, https://doi.org/10.5194/essd-8-297-2016.

Orsi W D, Smith J M, Liu S T, Liu Z F, Sakamoto C M, Wilken S, Poirier C, Richards T A, Keeling P J, Worden A Z, Santoro A E. 2016. Diverse, uncultivated bacteria and archaea underlying the cycling of dissolved protein in the ocean. *ISME Journal*, **10**(9): 2158-2173, https://doi.org/10.1038/ismej.2016.20.

Park P K. 1969. A practical handbook of seawater analysis. Fisheries Research Board of Canada Bulletin 167. J. D. H. Strickland, T. R. Parsons. *The Quarterly Review of Biology*, **44**(3): 327.

Park S J, Kim J G, Jung M Y, Kim S J, Cha I T, Ghai R, Martín-Cuadrado A B, Rodríguez-Valera F, Rhee S K. 2012. Draft genome sequence of an ammonia-oxidizing archaeon, "*Candidatus Nitrosopumilus sediminis*" AR2, from Svalbard in the Arctic Circle. *Journal of Bacteriology*, **194**(24): 6948-6949, https://doi.org/10.1128/JB.01869-12.

Pereira O, Hochart C, Auguet J et al. 2019. Genomic ecology of Marine Group II, the most common marine planktonic Archaea across the surface ocean. *MicrobiologyOpen*, **8**(9): e00852, https://doi.org/10.1002/mbo3.852.

Pester M, Schleper C, Wagner M. 2011. The Thaumarchaeota: an emerging view of their phylogeny and ecophysiology. *Current Opinion in Microbiology*, **14**(3): 300-306, https://doi.org/10.1016/j.mib.2011.04.007.

Picard A, Daniel I. 2013. Pressure as an environmental parameter for microbial life—a review. *Biophysical Chemistry*, **183**: 30-41, https://doi.org/10.1016/j.bpc.2013.06.019.

Pielou E C. 1966. The measurement of diversity in different types of biological collections. *Journal of Theoretical Biology*, **13**: 131-144, https://doi.org/10.1016/0022-5193(66)90013-0.

Pires A C C, Cleary D F R, Almeida A, Cunha Â, Dealtry S, Mendonça-Hagler L C S, Smalla K, Gomes N C M. 2012. Denaturing gradient gel electrophoresis and barcoded pyrosequencing reveal unprecedented archaeal diversity in mangrove sediment and rhizosphere samples. *Applied and Environmental Microbiology*, **78**(16): 5520-5528, https://doi.org/10.1128/AEM.00386-12.

Pommier T, Canbäck B, Riemann L, Boström K H, Simu K, Lundberg P, Tunlid A, Hagström Å. 2007. Global patterns of diversity and community structure in marine bacterioplankton. *Molecular Ecology*, **16**(4): 867-880, https://doi.org/10.1111/j.1365-294X.2006.03189.x.

Price M N, Dehal P S, Arkin A P. 2009. FastTree: computing large minimum evolution trees with profiles instead of a distance matrix. *Molecular Biology and Evolution*, **26**(7): 1641-1650, https://doi.org/10.1093/molbev/msp077.

Qian G, Wang J, Kan J J, Zhang X D, Xia Z Q, Zhang X C, Miao Y Y, Sun J. 2018. Diversity and distribution of anammox bacteria in water column and sediments of the eastern Indian Ocean. *International Biodeterioration & Biodegradation*, **133**: 52-62, https://doi.org/1016/j.ibiod.2018.05.015.

Qin H M, Gao D K, Zhu M L, Li C, Zhu Z L, Wang H B, Liu W D, Tanokura M, Lu F P. 2020. Biochemical characterization and structural analysis of ulvan lyase from marine *Alteromonas* sp. reveals the basis for its salt tolerance. *International Journal of Biological Macromolecules*, **147**: 1309-1317, https://doi.org/10.1016/j.ijbiomac.2019.10.095.

Ramirez-Llodra E, Brandt A, Danovaro R, De Mol B, Escobar E, German C R, Levin L A, Arbizu P M, Menot L, Buhl-Mortensen P, Narayanaswamy B E, Smith C R, Tittensor D P, Tyler P A, Vanreusel A, Vecchione M. 2010. Deep, diverse and definitely different: unique attributes of the world's largest ecosystem. *Biogeosciences*, **7**(9): 2851-2899, https://doi.org/10.5194/bg-7-2851-2010.

Reintjes G, Tegetmeyer H E, Bürgisser M, Orlić S, Tews I, Zubkov M, Voß D, Zielinski O, Quast C, Glöckner F O, Amann R, Ferdelman T G, Fuchs B M. 2019. On-site analysis of bacterial communities of the ultraoligotrophic south Pacific gyre. *Applied and Environmental Microbiology*, **85**(14): e00184-19, https://doi.org/10.1128/AEM.00184-19.

Rosling A, Cox F, Cruz-Martinez K, Ihrmark K, Grelet G A, Lindahl B D, Menkis A, James T Y. 2011. Archaeorhizomycetes: unearthing an ancient class of ubiquitous soil fungi. *Science*, **333**(6044): 876-879, https://doi.org/10.1126/science.1206958.

Rosling A, Timling I, Taylor L. 2013. Archaeorhizomycetes: patterns of distribution and abundance in soil. *In*: Horwitz B, Mukherjee P, Mukherjee M, Kubicek C eds. Genomics of Soil- and Plant-Associated Fungi. Springer, Berlin, Heidelberg. p.333-349, https://doi.org/10.1007/978-3-642-39339-6_14.

Sayed A M, Hassan M H A, Alhadrami H A, Hassan H M, Goodfellow M, Rateb M E. 2020. Extreme environments: microbiology leading to specialized metabolites. *Journal of Applied Microbiology*, **128**(3): 630-657, https://doi.org/10.1111/jam.14386.

Segata N, Izard J, Waldron L, Gevers D, Miropolsky L, Garrett W S, Huttenhower C. 2011. Metagenomic biomarker discovery and explanation. *Genome Biol.*, **12**: R60, https://doi.org/10.1186/gb-2011-12-6-r60.

Shannon C E. 1948. A mathematical theory of communication. *The Bell System Technical Journal*, **27**(4): 623-656, https://doi.org/10.1002/j.1538-7305.1948.tb00917.x.

Simpson E H. 1949. Measurement of diversity. *Nature*, **163**(4148): 688, https://doi.org/10.1038/163688a0.

Singh P, Raghukumar C, Verma P, Shouche Y. 2011. Fungal community analysis in the deep-sea sediments of the central Indian basin by culture-independent approach. *Microbial Ecology*, **61**(3): 507-517, https://doi.org/10.1007/s00248-010-9765-8.

Sinha R K, Krishnana K P, Thomas F A, Binish M B, Mohan M, Kurian P J. 2019. Polyphasic approach revealed complex bacterial community structure and function in deep sea sediment of ultra-slow spreading Southwest Indian Ridge. *Ecological Indicators*, **96**: 50-51, https://doi.org/10.1016/j.ecolind.2018.08.063.

Sunagawa S, Coelho L P, Chaffron S, Kultima J R, Labadie K, Salazar G, Djahanschiri B, Zeller G, Mende D R, Alberti A, Cornejo-Castillo F M, Costea P I, Cruaud C, d'Ovidio F, Engelen S, Ferrera I, Gasol J M, Guidi L, Hildebrand F, Kokoszka F, Lepoivre C, Lima-Mendez G, Poulain J, Poulos B T, Royo-Llonch M, Sarmento H, Vieira-Silva S, Dimier C, Picheral M, Searson S, Kandels-Lewis S, Tara Oceans coordinators, Bowler C, de Vargas C, Gorsky G, Grimsley N, Hingamp P, Iudicone D, Jaillon O, Not F, Ogata H, Pesant S, Speich S, Stemmann L, Sullivan M B, Weissenbach J, Wincker P, Karsenti E, Raes R, Acinas S G, Bork P. 2015. Structure and function of the global ocean microbiome. *Science*, **348**(6237): 1261359, https://doi.org/10.1126/science.1261359.

Sverdrup H U, Johnson M W, Fleming R H. 1942. The Oceans: Their Physics, Chemistry, and General Biology. Prentice-Hall, New York.

Uraibi H S, Midi H, Rana S. 2017. Selective overview of forward selection in terms of robust correlations.

Communications in Statistics - Simulation and Computation, **46**(7): 5479-5503, https://doi.org/10.1080/03610918.2016.1164862.

Wang J, Kan J J, Borecki L, Zhang X D, Wang D X, Sun J. 2016. A snapshot on spatial and vertical distribution of bacterial communities in the eastern Indian Ocean. *Acta Oceanologica Sinica*, **35**(6): 85-93, https://doi.org/10.1007/s13131-016-0871-4.

Wang Y Y, Liao S L, Gai Y B, Liu G L, Jin T, Liu H, Gram L, Strube M L, Fan G Y, Sahu S K, Liu S S, Gan S H, Xie Z X, Kong L F, Zhang P F, Liu X, Wang D Z. 2021. Metagenomic analysis reveals microbial community structure and metabolic potential for nitrogen acquisition in the oligotrophic surface water of the Indian Ocean. *Frontiers in Microbiology*, **12**: 518865, https://doi.org/10.3389/fmicb.2021.518865.

Wang Z P, Liu Z Z, Wang Y L, Bi W H, Liu L, Wang H Y, Zheng Y, Zhang L L, Hu S G, Xu S S, Zhang P. 2019. Fungal community analysis in seawater of the Mariana Trench as estimated by Illumina HiSeq. *RSC Advances*, **9**(12): 6956-6964, https://doi.org/10.1039/c8ra10142f.

Wemheuer F, von Hoyningen-Huene A J E, Pohlner M, Degenhardt J, Engelen B, Daniel R, Wemheuer B. 2019. Primary production in the water column as major structuring element of the biogeographical distribution and function of archaea in deep-sea sediments of the central Pacific Ocean. *Archaea*, **2019**: 3717239, https://doi.org/10.1155/2019/3717239.

White T J, Bruns T, Lee S, Taylor J. 1990. Amplification and direct sequencing of fungal ribosomal RNA genes for phylogenetics. *In*: PCR Protocols. Academic Press, London. p.315-322, https://doi.org/10.1016/B978-0-12-372180-8.50042-1.

Winter C, Matthews B, Suttle C A. 2013. Effects of environmental variation and spatial distance on bacteria, archaea and viruses in sub-polar and arctic waters. *ISME Journal*, **7**(8): 1507-1518, https://doi.org/10.1038/ismej.2013.56.

Xia X M, Guo W, Liu H B. 2017. Basin scale variation on the composition and diversity of archaea in the Pacific Ocean. *Frontiers in Microbiology*, **8**: 2057, https://doi.org/10.3389/fmicb.2017.02057.

Xu W, Pang K L, Luo Z H. 2014. High fungal diversity and abundance recovered in the deep-sea sediments of the Pacific Ocean. *Microbial Ecology*, **68**(4): 688-698, https://doi.org/10.1007/s00248-014-0448-8.

Yang C Y, Li Y, Zhou B, Zhou Y Y, Zheng W, Tian Y, Van Nostrand J D, Wu L Y, He Z L, Zhou J Z, Zheng T L. 2015. Illumina sequencing-based analysis of free-living bacterial community dynamics during an *Akashiwo sanguine* bloom in Xiamen Sea, China. *Scientific Reports*, **5**: 8476, https://doi.org/10.1038/srep08476.

Yao M R, Gao G P, Philips H E, Hu D H. 2017. Hydrographic features and water masses of southeast Indian Ocean region. *Journal of PLA University of Science and Technology* (*Natural Science Edition*), **18**(2): 170-176, https://doi.org/10.12018/j.issn.1009-3443.20170115001. (in Chinese with English abstract)

Yoshida K, Takano K, Teramoto T, Toba Y, Nagata Y, Kajiura K, Nannichi T, Iwata N, Takahashi T, Chaen M, Tabata T. 1971. Physical oceanography. *Journal of the Oceanographical Society of Japan*, **27**(6): 248-264, https://doi.org/10.1007/BF02109744.

Zhao Q Q, Bai J H, Gao Y C, Zhao H X, Zhang G L, Cui B S. 2020. Shifts in the soil bacterial community along a salinity gradient in the Yellow River Delta. *Land Degradation and Development*, **31**(16): 2255-2267, https://doi.org/10.1002/ldr.3594.

Electronic supplementary material

Supplementary material (Supplementary Tables S1–S8 and Figs.S1–S2) is available at https://doi.org/10.1007/s00343-021-1046-5.